Quantum breathing mode of interacting particles in harmonic traps

Sebastian Bauch, David Hochstuhl, Karsten Balzer, and Michael Bonitz

Institut für Theoretische Physik und Astrophysik, Christian-Albrechts-Universität Kiel, Leibnizstrasse 15, 24098 Kiel, Germany

E-mail: `bauch@theo-physik.uni-kiel.de`

Abstract. The breathing mode — the uniform radial expansion and contraction of a system of interacting particles — is analyzed. Extending our previous work [Bauch et al 2009 *Phys. Rev. B.* **80** 054515] we present a systematic analysis of the breathing mode for fermions with an inverse power law interaction potential $w(r) \sim r^{-d}$ with $d = 1, 2, 3$ in the whole range of coupling parameters. The results thus cover the range from the ideal "gas" to the Wigner crystal-like state. In addition to exact results for two particles obtained from a solution of the time-dependent Schrödinger equation we present results for $N = 4, 6$ from multiconfiguration time-dependent Hartree-Fock simulations.

1. Introduction

Quantum systems in traps and their time-dependent properties are of growing interest in many fields, including correlated electrons in metal clusters [1] or quantum dots [2, 3, 4] and ultracold Bose and Fermi gases in traps or optical lattices, for recent overviews see e.g. [5, 6]. Particular attention has recently been devoted to Bose-Einstein condensation in low dimensions [7] and to the analysis of nonideality (interaction) effects [8, 9, 10, 11], including superfluidity and crystallization, see [12].

In the case of strong coupling, the collective static and dynamic properties of these systems are largely determined by their collective modes [8, 9, 6]. It was shown in a recent paper [13] that, among them, the monopole or breathing mode (BM) which is easily excited experimentally [9] carries particularly valuable information on the system dimensionality d, the spin statistics of the particles and on the form and relative strength λ_d of their pair interaction given by Eqs. (4, 7-9).

In [13], the authors concentrated on the case of Coulomb interaction. Here, this analysis is extended to a more general interaction potential of inverse power form, $w(r) \sim r^{-d}$. In particular, new numerical results are presented for the cases $d = 2$ and $d = 3$. Moreover, the previous exact results were limited to two particles whereas for $N = 3$ and $N = 4$ time-dependent Hartree-Fock calculations were performed. Here we report results for $N \leq 6$ from Multiconfiguration Time-dependent Hartree-Fock calculations (MCTDHF) which include correlation corrections to the mean-field case.

The paper is organized as follows: first we introduce the system under consideration and our approach to model the basic properties of interacting trapped particles at arbitrary coupling by

means of solving the two-particle time-dependent Schrödinger equation in one spatial dimension. Following the discussion of the excitation and (theoretical) measurement of the collective modes in such a quantum system we switch to the case of $1/r^2$ interaction. Here, analytical results for the breathing mode offer profound benchmarks for our approach. We then investigate the fundamental cases of Coulomb and dipole interacting particles within a broad range of coupling strengths in detail and apply MCTDHF methods for more than two particles. We close with a conclusion and an outlook for further calculations, addressing the open questions arising from our work.

2. Model and solution procedure

Let us consider a system of N interacting particles in a harmonic trapping potential. The time-dependent Schrödinger equation (TDSE) for such a system reads

$$i\hbar \frac{\partial}{\partial t} \Psi(\boldsymbol{r}_1, ..., \boldsymbol{r}_N) = \hat{H} \Psi(\boldsymbol{r}_1, ..., \boldsymbol{r}_N, t), \tag{1}$$

with the N-particle Hamilton operator, given by

$$\hat{H} = \sum_{i=1}^{N} \hat{h}_i + \sum_{i \neq j}^{N} w(|\boldsymbol{r}_i - \boldsymbol{r}_j|) . \tag{2}$$

The single-particle hamiltonian, $\hat{h}_i$, is defined as the sum of the kinetic energy and the external single particle potential,

$$\hat{h}_i = \hat{t}_i + v_i(\boldsymbol{r}_i) . \tag{3}$$

The interaction is given by a binary interaction potential, depending on the distance of particle i and j,

$$w(|\boldsymbol{r}_i - \boldsymbol{r}_j|) = \frac{a_d}{|\boldsymbol{r}_i - \boldsymbol{r}_j|^d} , \tag{4}$$

with a d-dependent interaction parameter a_d (e.g. $a_1 = e^2/4\pi\epsilon_0$). Finally, one arrives at

$$i\hbar \frac{\partial}{\partial t} \Psi(\boldsymbol{r}_1, \ldots, \boldsymbol{r}_N; t) = \left(\frac{1}{2m} \sum_i \hat{P}_i^2 + \frac{1}{2} m\Omega^2 \sum_i \boldsymbol{r}_i^2 + a_d \sum_{i<j} \frac{1}{|\boldsymbol{r}_i - \boldsymbol{r}_j|^d} \right) \Psi(\boldsymbol{r}_1, \ldots, \boldsymbol{r}_N; t) . \tag{5}$$

We will concentrate on identical particles of equal masses, charges, dipole moments and spin projections in this work.

We now introduce scaled quantities, $\tilde{\boldsymbol{r}}_i = \sqrt{\frac{m\Omega}{\hbar}} \boldsymbol{r}_i$, $\tilde{\boldsymbol{P}}_i = \sqrt{\frac{1}{m\hbar\Omega}} \boldsymbol{P}_i$ and $\tilde{t} = t/\Omega$, which correspond to a rescaling of lengths, times and energies ($\tilde{E} = E/\hbar\Omega$). With the spatial coordinate representation of $\tilde{p}_i = -i\frac{\partial}{\partial \tilde{\boldsymbol{r}}_i}$ and omitting the tilde symbol in the following, we arrive at the dimensionless form of Eq. (5):

$$i\frac{\partial}{\partial t} \Psi(\boldsymbol{r}_1, \ldots, \boldsymbol{r}_N; t) = \left(-\frac{1}{2} \sum_i \frac{\partial^2}{\partial \boldsymbol{r}_i^2} + \sum_i \boldsymbol{r}_i^2 + \underbrace{\frac{ma_d}{\hbar^2} l_0^{2-d}}_{\lambda_d} \sum_{i<j} \frac{1}{|\boldsymbol{r}_i - \boldsymbol{r}_j|} \right) \Psi(\boldsymbol{r}_1, \ldots, \boldsymbol{r}_N; t) , \tag{6}$$

where λ_d is the interaction parameter, which contains all physical constants occurring in Eq. (5). For the cases considered in this work, we obtain:

(i) Coulomb interaction:

$$\lambda_1 = \frac{e^2}{4\pi\epsilon_0} \frac{m}{\hbar^2} \cdot l_0 \tag{7}$$

(ii) inverse square interaction:

$$\lambda_2 = a_2 \frac{m}{\hbar^2} \tag{8}$$

(iii) and dipole interaction:

$$\lambda_3 = a_3 \frac{m}{\hbar^2} \cdot \frac{1}{l_0} \tag{9}$$

with the oscillator length $l_0 = \sqrt{\hbar/m\Omega}$. The parameter λ_d describes the coupling of the system, i. e., the relative interaction strength between the particles, which can be tuned in experiments, e. g. by changing the frequency of the external trapping potential. We note here, that for $d = 2$ λ_2 is independent of l_0 and thus independent of Ω. Therefore, other physical parameters need to be changed (e.g. charge, mass, ...) in order to vary the interaction strength.

2.1. Breaking down to a two-particle problem
It has been shown for classical systems, corresponding to the case of $\lambda \to \infty$, that a purely radial and uniform breathing mode exists only in the following cases[14]:

(i) for clusters with special symmetries for any interaction

(ii) for every N if the interaction potential has the form $w(r) \propto 1/r^n$ or $w(r) \propto \log r$

Furtheron, it has been proven, that the classical breathing mode is *N-independent* (which is also true for the non-interacting quantum gas with $\lambda = 0$), which lets us conclude, that most of the properties should be present in the fundamental two-body problem. However, the independence of the breathing frequency on the particle number N is still an open question in the case of interacting quantum particles at intermediate coupling strengths which is addressed in the following section.

The TDSE for two interacting particles in a one-dimensional harmonic trap follows directly from Eq. (6) and reads as

$$i\frac{\partial}{\partial t}\Psi(x_1, x_2, t) = \left[-\frac{1}{2}\left(\frac{\partial^2}{\partial x_1^2} + \frac{\partial^2}{\partial x_2^2} \right) + \frac{r_1^2 + r_2^2}{2} + \frac{\lambda_d}{(x_1 - x_2)^d} \right]\Psi(x_1, x_2, t) \,. \tag{10}$$

To avoid divergencies in this low-dimensional system, the interaction potential needs to be regularized. We follow the "standard" procedure by using the soft-core potential

$$w(x_1, x_2) = +\frac{\lambda_d}{[(x_1 - x_2)^2 + \kappa^2]^{d/2}} \,, \tag{11}$$

with a small cut-off parameter κ. A brief remark on the influence of this parameter on our results is given below in section 3.1 in the discussion of the $1/r^2$ potential. A more detailed discussion, also addressing the influence on different states (antisymmetric/symmetric), is to be found in [13]. We may conclude here, that our results do not significantly depend on the special choices of κ, and are thus relevant for the limiting case of $\kappa \to 0$.

Obviously, the two-particle problem can be simplified to a (coupled system) of two ODEs, by transformation to (rescaled) center of mass and relative coordinates and utilizing a product ansatz $\Psi(R, r; t) = \phi(R/\sqrt{2}; t) \cdot \varphi(\sqrt{2}r; t)$ for the wave function. In one spatial dimension, one finally obtains

$$i\partial_t \phi(R, t) = \left(-\frac{1}{2}\frac{\partial^2}{\partial R^2} + \frac{R^2}{2} \right)\phi(R, t) \tag{12}$$

for the scaled center of mass problem and

$$i\partial_t \varphi(r,t) = \left(-\frac{\partial^2}{2\partial r^2} + \frac{1}{2}r^2 + \frac{\lambda_d}{2^{d/2}r^d} \right) \varphi(r,t) \tag{13}$$

for the TDSE of the scaled relative part of the wave function. This already indicates the occurrence of two types of motions — one class of (interaction-dependent) oscillations governed by the TDSE of the relative problem, Eq. (13), in the following indicated with ω_r and one for the (interaction-independent) center of mass problem, labeled by ω_R. However, the general version of the splitting involves a time-dependent constant which couples both modes, and it is not clear from the beginning, if this mode coupling introduces additional spectral features. For an illustration of the time-dependent density, see the supplementary video to ref.[13]. Therefore, the full two-particle TDSE, Eq. (10), is solved numerically by using a grid-based Crank-Nicolson approach in combination with operator-splitting for the time evolution.

2.2. Initial state and excitation of the breathing mode
We initially prepare the system in its anti-symmetric ground sate, i. e. the energetically lowest state with a wave function obeyeing $\Psi(x_1, x_2, t = 0) = -\Psi(x_2, x_1, t = 0)$. This corresponds to a system of two spin-polarized fermions. However, for 1D systems with our type of interaction (singular at $x_1 = x_2$ besides the smoothing by κ), the Bose-Fermi-mapping is applicable and our results hold also for bosonic systems [15]. The symmetry of the wave function is, of course, preserved during (real) time propagation of the TDSE. For different types of interactions and interaction parameters λ, this initial state is obtained by propagating the full two-particle TDSE in imaginary time.

To excite the radial mode, we switch off the external trap. Then, the interaction and the quantum mechanical dispersion (especially in the case of small λ) drive the particles out of their equilibrium position during TDSE propagation in real time. After a short period of time (typically $t_\text{off} = 0.1$) the trap is restored and the breathing mode is excited. This type of excitation is completely radial, and therefore no dipole moment is induced (which would lead to a dipole or sloshing/Kohn mode of frequency Ω in the observable $\langle x \rangle(t)$, cf. Appendix). The special choice of t_off and the explicit switching procedure (e.g. smooth or instantaneously) play no significant role and do no affect the resulting breathing oscillations, cf. [13] for a detailed investigation including also other types of (time-dependent) excitations.

2.3. Observing the breathing mode
The breathing mode manifests in a characteristic oscillation of an adequate observable, which has to be sensitive on monopole oscillations. Among others, one possible quantity is the expectation value of x^2, which corresponds in our case to the expectation value of the potential energy. This quantity measures the width $\langle \langle x^2 \rangle - \langle x \rangle \rangle (t)$ of the density in the trap, since the linear term $\langle x \rangle$ is absent owing to the vanishing dipole moment. An alternative approach is the calculation of $\langle |x| \rangle$ used as an observable in experiments on classical systems in [16]. However, the results for the breathing frequencies are the same [13]. We will only consider the case of $\langle x^2 \rangle(t)$ in the present work.

To extract the breathing frequencies ω_r and ω_R, we used a fitting procedure, which involves two independent frequencies:

$$f(t, \omega_r, \omega_R) = a \sin[\omega_R(t - t_0)] + b \sin[\omega_r(t - t_0')] + c \,. \tag{14}$$

The frequency ω_R related to the center of mass wave function has been fixed to the known exact analytical value of $\omega_R = 2$ which agrees perfectly with our simulation data. Thus, the existence of both modes results in a clearly visible beating in the time series of the potential energy in the simulation.
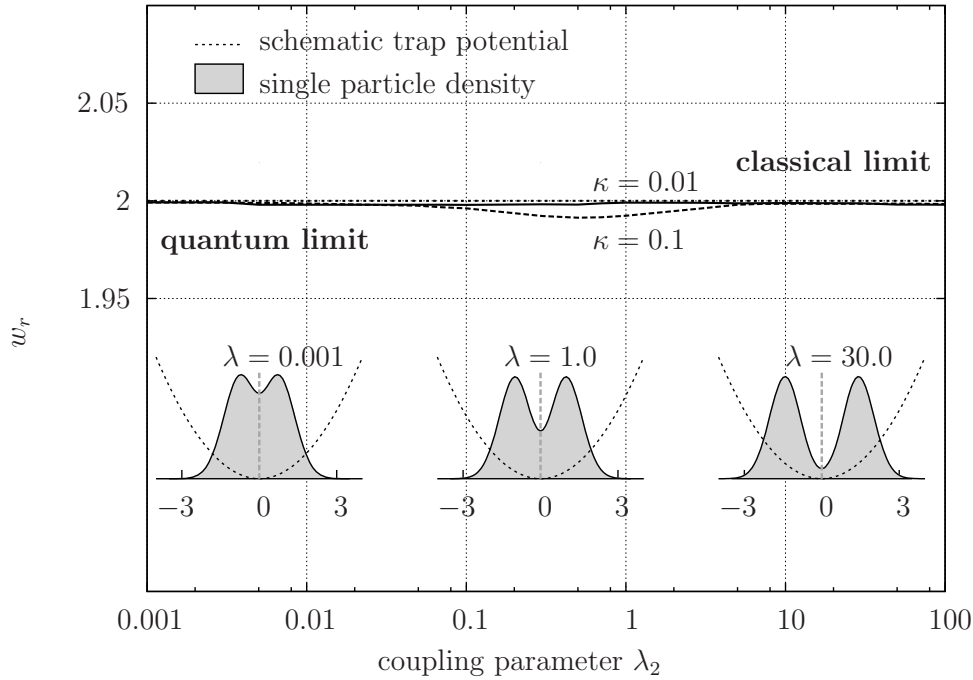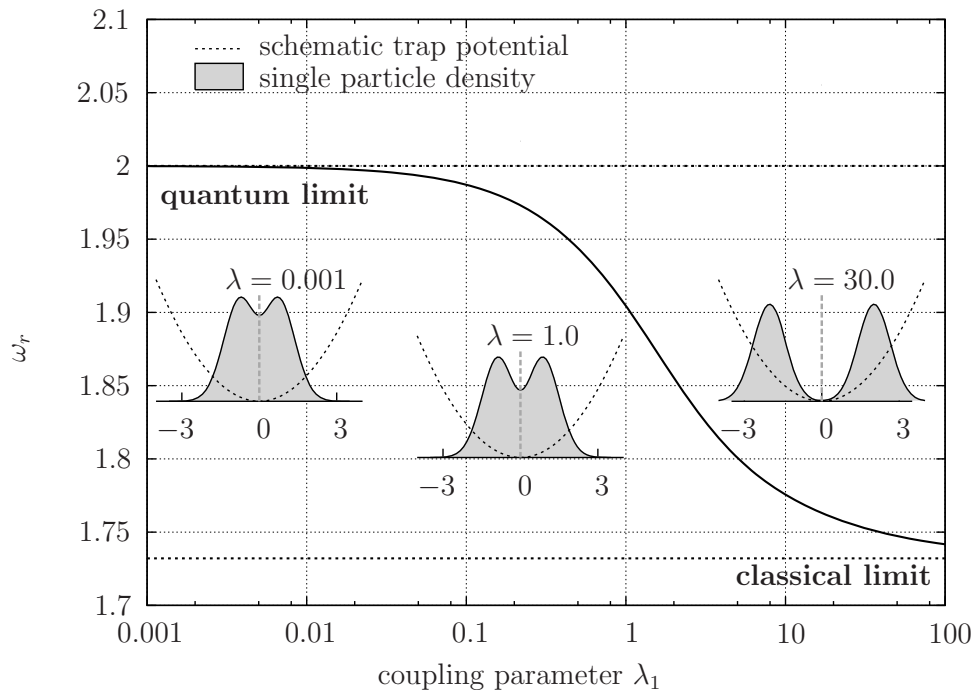
Figure 1. Breathing mode of two interacting particles in a harmonic trap for $1/r^2$ interaction. Shown is the mode ω_r associated with the relative wave function for two different values of the interaction smoothing parameter κ, cf. Eq. (11). The insets show the single-particle density (grey marked area) in the trap (schematically drawn by dashed lines), prior to excitation of the breathing mode for three different coupling regimes. The breathing mode is excited by turning off the trap for a duration of $t_{\text{off}} = 0.1$ and measuring the oscillation of $\langle x^2 \rangle(t)$. The mode associated with the center-of-mass problem, $\omega_R = 2$, is not shown.

3. Results for two particles

3.1. $1/r^2$ interaction

The breathing modes in a many-particle system interacting via a $1/r^2$ potential are well known, both classically and in quantum mechanics. The corresponding frequency (of the relative mode) ω_r is independent of the coupling parameter λ and attains the universal value of $\omega_r = 2$ [17] which coincides with the pure quantum mode ω_R, being also independent of λ. Furtheron, the full N-particle spectrum in a one-dimensional trap has been calculated analytically [19]. Therefore, this special type of particle-particle interaction is a useful and powerful test for the methods, for the preparation of the initial state via imaginary time propagation (accuracy) as well as for the time-propagation yielding the collective modes. The results obtained provide a powerful benchmark which then can be generalized to other types of interaction ($d \neq 2$).

The results from our TDSE calculations are shown in Figure 1 for two values of the (necessary) regularization parameter κ. According to [17], the exact solution *without* κ is λ-independent. However, due to the potential smoothing for $\kappa = 0.1$ we find a slight modification at intermediate coupling (smaller than one percent) which drops if one decreases κ further. That lets us conclude, that calculations with antisymmetric (spin-polarized) wave functions give the correct value for the breathing frequency — also in the case of other types of interactions, cf. [13] for a discussion concerning symmetric initial states. Figure 1 also gives the calculated single-particle densities before excitation of the breathing modes, obtained by imaginary time propagation for three chosen values of λ. One clearly sees the transition from a delocalized quantum state ($\lambda = 0.001$) with large overlap of both density peaks to a state with well-separated densities, corresponding

Figure 2. Breathing mode of two Coulomb interacting particles in a harmonic trap. All parameters are as in Fig. 1.

to a classical-like behavior ($\lambda = 30$).

3.2. Coulomb interaction

The second case is the Coulomb type interaction, $d = 2$. Figure 2 shows the result for $\omega_r(\lambda)$ for two particles in a harmonic trap. Both known limits, the quantum limit $\omega_r = 2$ of the non-interacting quantum gas and the classical case, $\omega = \sqrt{3}$ are indicated by dotted lines. With increasing λ, the mode ω_r decreases towards the classical regime. In between both limits, a smooth monotonic transition from the non-interacting to the strongly-coupled case is to be found. In analogy to the previous case, the single-particle densities in the trap are shown for the different interaction regimes, showing the same trend as in the $1/r^2$ case: for the ideal system, the double-peak structure in the single-particle density of two spin-polarized fermions in a harmonic trap is retrieved, whereas in the limit of large λ, the density separates into two distinct peaks being of perfect Gaussian shape exhibiting no significant overlap.

3.3. Dipole interaction

The case of dipole interaction, $d = 3$, is important for the investigation of dipolar quantum gases in traps and/or electron-hole bilayers [12, 18]. The classical value is known to be $\omega_r = \sqrt{5}$ whereas the quantum limit for $\lambda = 0$ is again $\omega_r = 2$. The result for two particles in a harmonic trap is given in Figure 3. One again recognizes the smooth, monotonic transition from the non-interacting to the classical regime. In contrast to Coulomb, the breathing mode ω_r increases with stronger interaction. For $\lambda = 100$, the classical case is not yet reached, in contrast to the case of Coulomb interaction. The explanation is to be found in the densities. In the case of dipole interaction, the density peaks have a non-vanishing overlap also in the case of large λ (case $\lambda = 30$ shown), which is not the case for Coulomb interaction, cf. Fig. 2 $\lambda = 30.0$. Therefore, the classical-like regime is reached only for larger λ. We note, that calculations for larger values
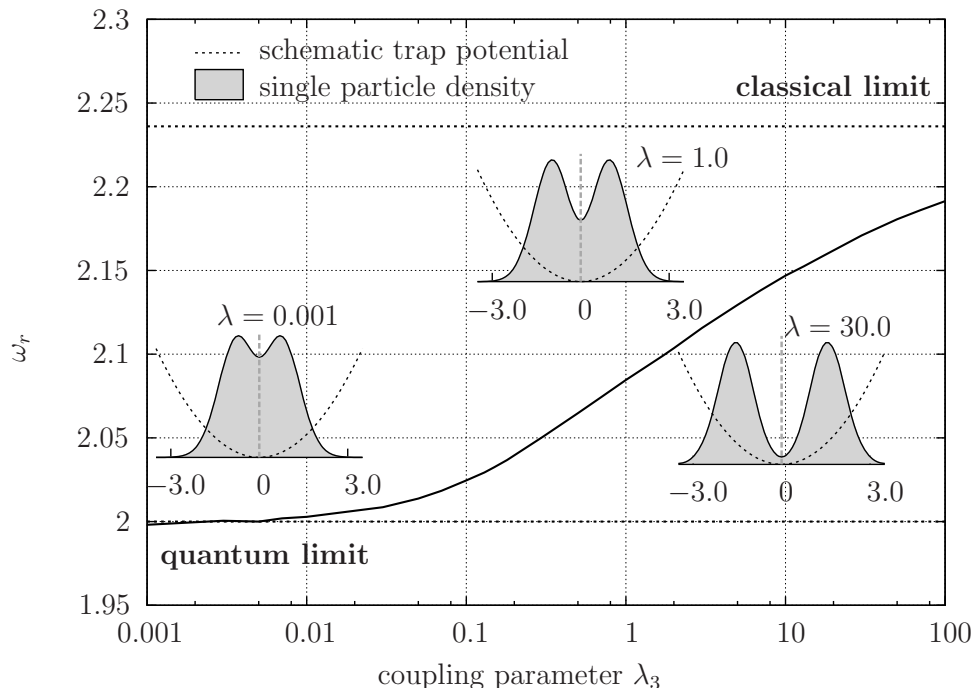
Figure 3. Breathing mode of two dipole interacting particles in a harmonic trap. All parameters are as in Fig. 1.

of λ become very demanding, because the potential gets very steep and the necessary numerical grid to represent the wave function (and the potentials) needs to be very fine.

Figure 4 shows a comparison of the breathing behavior for Coulomb and dipole systems, where the appropriate parameter for comparison is the oscillator length l_0, cf. Eqs. (7) and (9). In this representation, the differences of Coulomb and dipole interacting particles become apparent: whereas for Coulomb interaction the high density regime (small l_0) corresponds to small λ (ideal quantum gas) and the low density regime (large l_0) behaves classically, the opposite is true for dipole interaction. Here, the ideal quantum regime is observed for low density whereas the case of strong coupling corresponding to well-separated, classically behaving particles, occurs at high densities.

4. Larger particle numbers

To investigate the behavior of the breathing mode related to the relative problem for more than two particles, we performed time-dependent multi-configuration Hartree-Fock simulations, where the inclusion of correlation effects can be tuned via a parameter M determining the involved Slater determinants to represent the N-particle wave function. For a detailed description of the method and references for further reading, see [20] and [21] in the present volume. We concentrate on the fundamental case of Coulomb interaction ($d = 1$) in the following. Figure 5 shows the result for the relative breathing frequency, ω_r for up to $N = 6$ particles obtained via the multi-configuration Ansatz. The correlation parameter M has been adjusted to $M = N + 2$ to account for correlation beyond the mean-field Hartree-Fock level. The
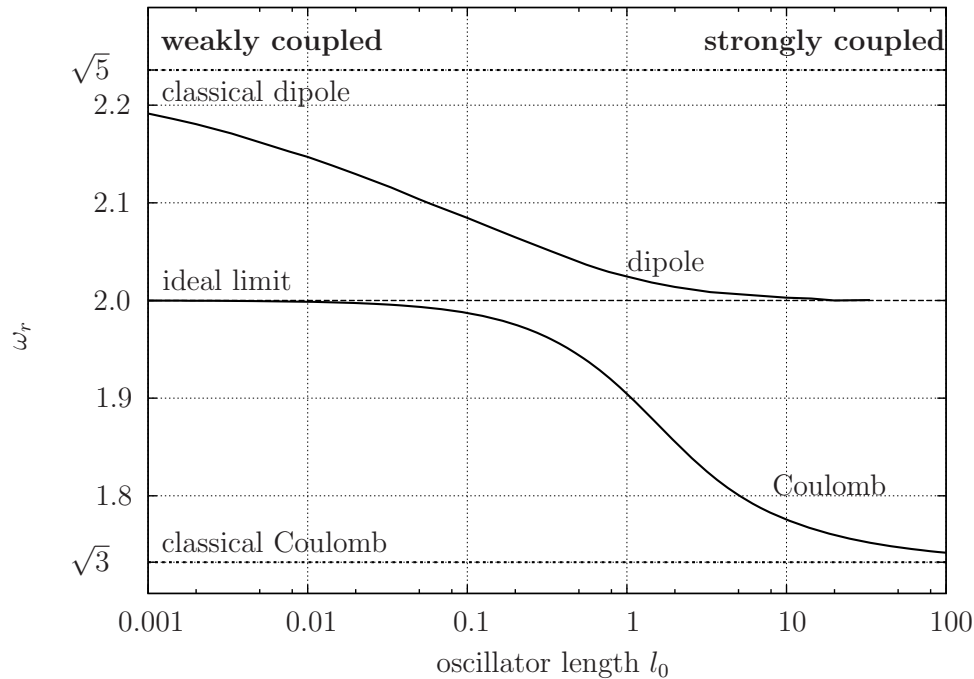
Figure 4. Breathing mode of two interacting (dipole/Coulomb interaction) particles in a harmonic trap plotted vs. characteristic length scale l_0. The regimes of strong and weak coupling are indicated.

comparison with the TDSE result for two particles (bold black line) shows perfect agreement with the MCTDHF calculations for two particles. However, for larger particle numbers, additional Slater determinants are needed, thus the degree of included correlations differs for different particle numbers. The inspection of the λ_1 dependence of ω_r reveals a N-independent shape, a smooth transition from the weakly interacting quantum gas to the strongly coupled classical case. However, in the transition region of intermediate coupling a weak dependence on N can be spotted, but this might be due to additional correlation effects beyond the $M = N + 2$ approximation.

5. Conclusion and outlook

In summary, we have computed the breathing modes of interacting one-dimensional quantum systems for different types of interaction. In all cases, two different modes occur, one center-of-mass related breathing motion independent of the coupling of the particles, and one relative mode. The latter one can be identified as the classical-alike mode, which asymptotically attains in all investigated cases the classical value for the breathing frequency. Furtheron the dependence on the particle number has been investigated via the powerful, in general exact, multi-configurational Hartree Fock method revealing a similar structure of the dependence on the coupling of the breathing mode associated with the relative oscillation. However, the question whether the breathing mode is independent of the particle number for arbitrary coupling, as it is in the two limits, remains unanswered and is postponed to a forthcoming work.
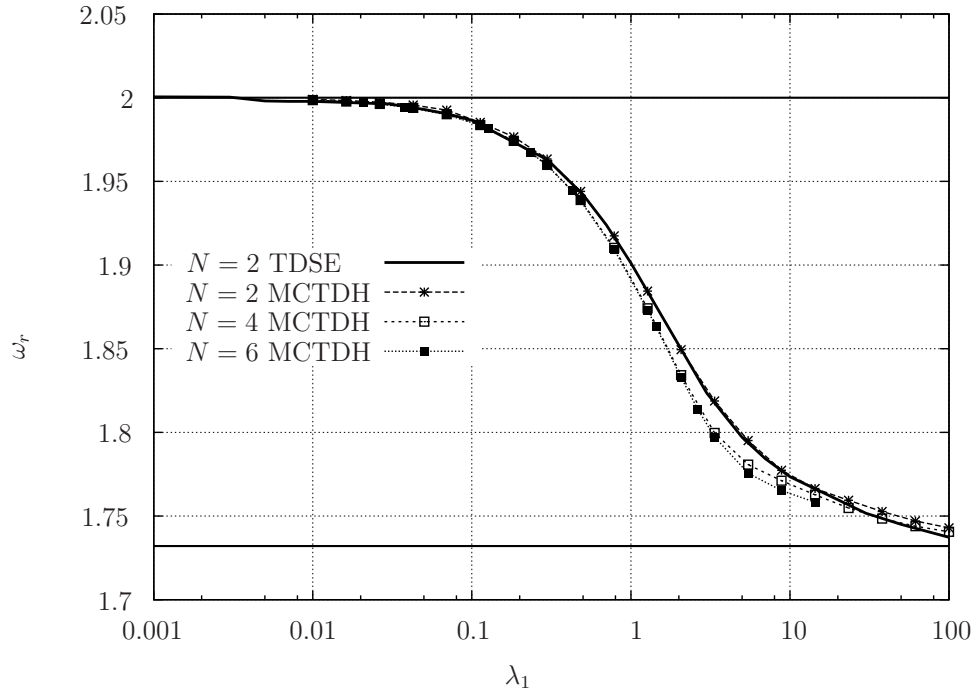
Figure 5. Dependence of the breathing mode associated with the relative motion, ω_r, on the particle number N for $N = 2, 4, 6$ Coulomb interacting particles in a harmonic trap. The results are obtained via the direct solution of the TDSE and via the multi-configuration Hartree Fock ansatz. The correlation tuning parameter M in the MCTDHF method has been set to $M = N + 2$.

Appendix A. Derivation of (ideal) breathing frequency $\omega_{\mathbf{R}}$

We consider the center of mass problem, cf. Eq. (12), in one spatial dimension, which is nothing else than a simple harmonic oscillator problem ($R \equiv x$):

$$i\partial_t \phi(x,t) = \left(-\frac{1}{2}\frac{\partial^2}{\partial x^2} + \frac{x^2}{2} \right) \phi(x,t) \ . \tag{A.1}$$

Any initial excitation, e. g. created by switching off the trap for a small period of time, can be written as a superposition of eigenstates ϕ_m,

$$\phi(x, t = 0) = \sum_m c_m \phi_m(x) \ , \tag{A.2}$$

where

$$\left(-\frac{1}{2}\frac{\partial^2}{\partial x^2} + x^2 \right) \phi_m = \left(m + \frac{1}{2} \right) \phi_m \ . \tag{A.3}$$

The (time-dependent) solution of Eq. (A.1) is then simply given by

$$\phi(x,t) = \sum_m c_m \phi_m(x) e^{-iE_m t} \ , \tag{A.4}$$

where $E_m = m + 1/2$ denotes the eigenvalues associated with the eigenfunction ϕ_m. The measurable quantities, giving the collective modes of the system, are physical observables of the

form $\langle x^k \rangle(t)$ for $k = 0, 1, ...$ Their time dependence follows as

$$\langle x^k \rangle(t) = \sum_{ij} c_i^* c_j e^{-i(E_j - E_i)t} (x^k)_{ij} \,, \tag{A.5}$$

with matrix elements $(x^k)_{ij} = \int \mathrm{d}x \phi_i^*(x) x^k \phi_j(x)$. Therefore, $\langle x^k \rangle(t)$ may oscillate with frequencies $\omega^{(k)} = |E_j - E_i|, i \neq j$, depending on the initial state c_i and the corresponding matrix elements $(x^k)_{ij}$.

We now consider only the relevant cases for k:

(i) $k = 1$ (*dipole moment*): the frequency for dipole oscillations is given by $\omega^{(1)} = 1$, because $(x)_{ij} \propto \delta_{ij} \pm 1$. This leads to the well-known Kohn (sloshing mode)

(ii) $k = 2$ (*potential energy*): $\langle x^2 \rangle(t)$ may oscillate with $\omega^{(2)} = 2$, since $(x^2)_{ij} \neq 0$ only for $i = j$ and $i = j \pm 2$.

For our type of radial excitation, no dipole moment is induced. Hence, only the second case is relevant, and the observable oscillation of the center of mass part of the two-particle wave function attains the λ-independent value of $\omega^{(2)} = \omega_R = 2$. As the derivation of the center-of-mass wave function is N-independent, also the oscillation of the non-interacting, ideal quantum gas behaves uniformly, in analogy to the case of the strongly coupled, classical case.

References

[1] Baletto F and Ferrando R 2005 *Rev. Mod. Phys.* **77** 371
[2] Filinov A V, Bonitz M and Lozovik Yu E 2001 *Phys. Rev. Lett.* **86** 3851
[3] Filinov A V, Lozovik Yu E and Bonitz M 2000 *Phys. Stat. Sol. (b)* **221** 231
[4] Reimann S M and Manninen M 2002 *Rev. Mod. Phys.* **74** 1283
[5] Bloch I 2005 *Nature Phys.* **1** 23
[6] Giorgini S, Pitaevskii L P and Stringari S 2008 *Rev. Mod. Phys.* **80** 1215
[7] Görlitz A, Vogels J M, Leanhardt A E, Raman C, Gustavson T L, Abo-Shaeer J R, Chikkatur A P, Gupta S, Inouye S, Rosenband T and Ketterle W 2001 *Phys. Rev. Lett.* **87** 130402
[8] Menotti C and Stringari S 2002 *Phys. Rev. A* **66** 043610
[9] Moritz H, Stöferle Th, Köhl M and Esslinger T 2003 *Phys. Rev. Lett.* **91** 250402
[10] Pedri P, De Palo S, Orignac E, Citro R and Chiofalo M K 2008 *Phys. Rev. A* **77** 015601
[11] Bloch I, Dalibard J, Zwerger W 2008 *Rev. Mod. Phys.* **80** 885
[12] Filinov A, Böning J, Bonitz M and Lozovik Yu E 2008 *Phys. Rev. B* **77** 214527
[13] Bauch S, Balzer K, Henning C and Bonitz M 2009 *Phys. Rev. B* **80** 054515
[14] Henning C, Fujioka K, Ludwig P, Piel A, Melzer A and Bonitz M 2008 *Phys. Rev. Lett.* **101** 045002
[15] Girardeau M 1960 *J. Math. Phys.* **1** 516
[16] Melzer A, Klindworth M and Piel A 2001 *Phys. Rev. Lett.* **87** 115002
[17] Geller M R and Vignale G 1996 *Phys. Rev. B* **53** 6979
[18] Filinov A, Ludwig P, Bonitz M, and Lozovik Yu E 2009 *J. Phys. A* **42** 214016
[19] Calogero F 1971 *J. Math. Phys.* **12** 419
[20] Bonitz M, Hochstuhl D, Bauch S, and Balzer K 2010 *Contrib. Plasma Phys.* **80** 54–59
[21] Hochstuhl D, Bauch S and Bonitz M 2009 Proceedings of conference PNGF IV this issue